



# Growth of Robinson tilings

Daria Pchelina

August, 2018

## 1 Introduction

A **Wang tile** is a unit square with colored edges, such as: ; a set of Wang tiles is called a **tileset**. A **tiling of the plane** by a tileset  $A$  is a covering of the plane with translated copies of tiles from  $A$ . A tiling of the plane is called **valid** if for any pair of neighboring tiles, their adjacent edges have the same color as, for instance, in: . Figure 1 shows an example of a tileset and a valid tiling by this tileset.

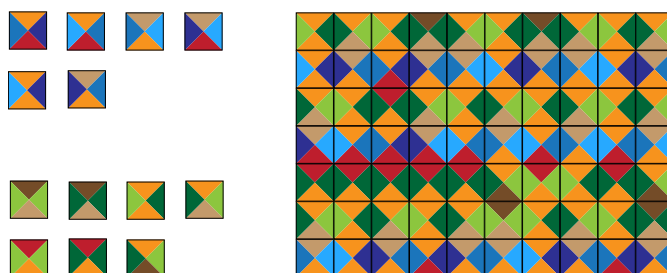


Figure 1: Example of a tileset and of a valid tiling.

These tiles were introduced by Hao Wang in 1961 [13] as a simple combinatorial problem: given a finite tileset  $A$ , decide whether there exists a valid tiling of the plane by  $A$ . It is called the Domino Problem. Wang conjectured that there exist no aperiodic tilesets (in other words, tilesets generating only aperiodic tilings of the plane); assuming this, he could find an algorithm solving the Domino Problem. However, 3 years later, Robert Berger [1] proved the Domino Problem to be undecidable and showed a counterexample to Wang's conjecture. Since then, researchers got involved in a kind of a "competition" for the smallest aperiodic Wang tileset [2, 8, 11]. This competition was over in 2015 when Jeandel and Rao found the smallest aperiodic tileset (11 tiles) and proved by an exhaustive search that there exist no smaller aperiodic tilesets [7].

Now Wang tiles are widely studied in the context of discrete dynamical systems, combinatorics, computability theory and geometry. However, in all of these areas, a tiling is considered as an object given a priori. There are also applications in chemistry and physics, but they require to study the process of creation of a given tiling; we call it growth.

There exist many processes in nature where tiny particles, forced by local conditions, assemble together in a large structure. Crystal growth and self-assembly of DNA molecules are the most common examples of this phenomenon. Tilings of the plane are a possible mathematical model for these processes; for instance, Wang tilings are used to simulate molecular growth [3]. In general, tiles could have non-square shapes with the same color-constraints mentioned above; for instance, Penrose tilings [6, 10] describe the behavior of quasicrystals. Socolar, in [12], formalized the notion of growth for Penrose tilings and, among other things, showed that starting with a specific configuration, such a tiling can cover the whole plane in a process of growth.

In 1971, Raphael Robinson introduced an aperiodic set of 32 square tiles; he used this tileset to design a simple and elegant proof of the undecidability of the Domino Problem [11]. This tileset is now classical and is used in recent constructions from information theory (for instance, to prove the existence of tilesets with high Kolmogorov complexity [4]).

As we have already mentioned, all tilings of the plane by the Robinson tiles are aperiodic. In other words, for any valid Robinson tiling  $\tau$  there exist no vector  $p \in \mathbb{Z}^2$  such that  $\tau(z) = \tau(z + p)$  for any  $z \in \mathbb{Z}^2$ . This holds because Robinson tilings have hierarchical (think: fractal) structure. Penrose tilings, whose growth has been studied before, also have hierarchical structure (but different from the Robinson's hierarchy). The first question that we could ask is: does hierarchy imply specific growth properties? Besides that, there exist many constructions based on the Robinson tileset, so after analysing its growth, we could easily expand the results to these constructions.

Here we study the question of growth for Robinson tilings; we simulate this process with cellular automata. It turns out that, by contrast with Penrose tilings [12], Robinson tilings can not grow in our model.

In Section 2, we explain the local rules and hierarchy of Robinson tilings. The formal definition of the growth of Robinson tilings is given in Section 3. In Section 4, we state the main result and prove it.

### 1.1 Preliminaries

Elements of  $\mathbb{Z}^2$  are called **cells**. Given a tileset  $A$ , a **tiling of the plane** is a function  $\mathbb{Z}^2 \rightarrow A$ . A tiling of  $D \subseteq \mathbb{Z}^2$  is a function  $D \rightarrow A$ , it is called a **configuration** of  $D$ . We denote a restriction of a configuration  $S : D \rightarrow A$  to a set  $F \subseteq D$  by  $S|_F$ .

Given a cell  $z$ , a square of size  $(2t + 1) \times (2t + 1)$  centered on  $z$  is called a **t-neighborhood** of  $z$  and is denoted by  $B_t(z)$ . Usually it is called the Moore neighborhood. (See Figure 2).

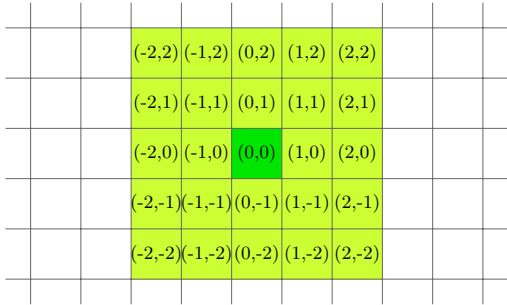


Figure 2: 2-neighborhood of the cell (0,0).

We define a **quadrant** with origin  $(x_0, y_0) \in \mathbb{Z}^2$  as a set  $Q_{x_0 y_0} = \{(x, y) \mid x \geq x_0, y \geq y_0\}$ <sup>1</sup>.

## 2 The Robinson tileset

The **Robinson tileset** is the set of 32 tiles obtained by rotations from the ones displayed on Figure 3. A piece of a Robinson tiling is displayed in Figure 4.

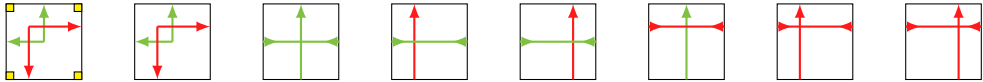


Figure 3: The Robinson tiles, up to rotation.

<sup>1</sup>We consider only north-east quadrants since the internship took place in the north-east

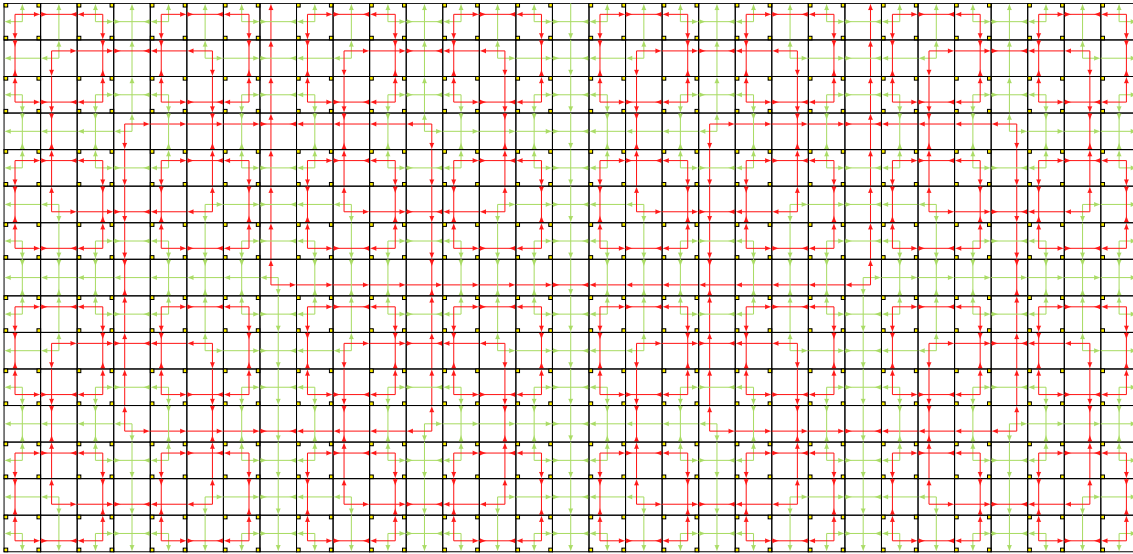


Figure 4: A piece of a Robinson tiling.

## 2.1 Local rules

The local rules for Robinson tiles, as they are displayed in Figure 3, are not quite color constraints. Instead, a tiling of the plane by Robinson tiles is **valid** if it satisfies the rules:

- ( $\rightarrow$ ) For any pair of neighbor tiles, arrows meeting at their adjacent edge have the same color, direction and position on the edge. (See Figure 5 for an example).
- ( $::$ ) Among any four tiles sharing a corner, exactly one has yellow dots in its corners. (See Figure 6 for an example).

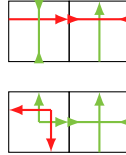


Figure 5: Valid pairs of adjacent tiles.

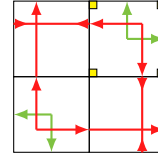


Figure 6: Four tiles sharing a corner.

It is possible to design a set of 56 Wang tiles equivalent to the Robinson tiling, but we won't do it here.

Given a configuration of  $D$  and a tile in this configuration, this tile is called **valid** in the configuration if each  $2 \times 2$ -square containing this tile satisfies the Robinson rules or can be extended to such square (if  $D$  doesn't contain one of these cells). A configuration is called valid if all its tiles are valid in it.

## 2.2 Hierarchy

We see red squares of different sizes in Figure 4, they appear in all Robinson tilings of the plane. We define four sequences of macrotiles  $a_n, b_n, c_n$  and  $d_n$  as follows. They will help us to analyze the hierarchy of Robinson tilings.

- Four tiles with yellow dots are called **macrotiles of rank 0**, they are denoted as  $a_0, b_0, c_0$  and  $d_0$  as shown in Figure 7.

- Each **macrotile of rank 1** is a  $3 \times 3$ -square, whose corner tiles are filled with  $a_0, b_0, c_0$  and  $d_0$  as shown in Figure 8. For any  $x \in \{a, b, c, d\}$ , the central cell of  $x_1$  is the same as  $x_0$  without dots, and the 4 remaining cells are filled with the only tiles valid for these positions.
- Suppose macrotiles of rank  $n$  are defined; they are  $(2^{n+1} - 1) \times (2^{n+1} - 1)$ -squares. Then each  **$(n + 1)$ -macrotile** is a  $(2^{n+2} - 1) \times (2^{n+2} - 1)$ -square, whose corners are filled by  $a_n, b_n, c_n$  and  $d_n$  in the same order as for 1-macrotiles. For any  $x \in \{a, b, c, d\}$ , the central cell of  $x_{n+1}$  is the same as  $x_0$  without dots, and the remaining cells forming a large cross are filled with the only possible tiles for these cells.

The detailed constructions of macrotiles  $a_1$  and  $a_2$  are shown in Figures 8, 9.

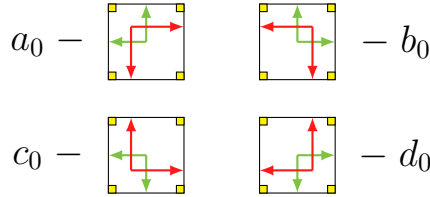


Figure 7: Robinson macrotiles  $a_0, b_0, c_0$  and  $d_0$ .

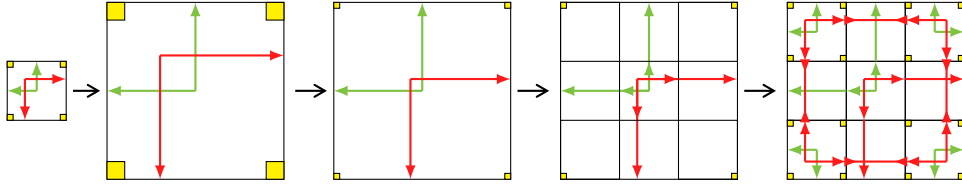


Figure 8: Transformation of a macrotile of level 0 ( $a_0$ ) in a macrotile of level 1 ( $a_1$ ).

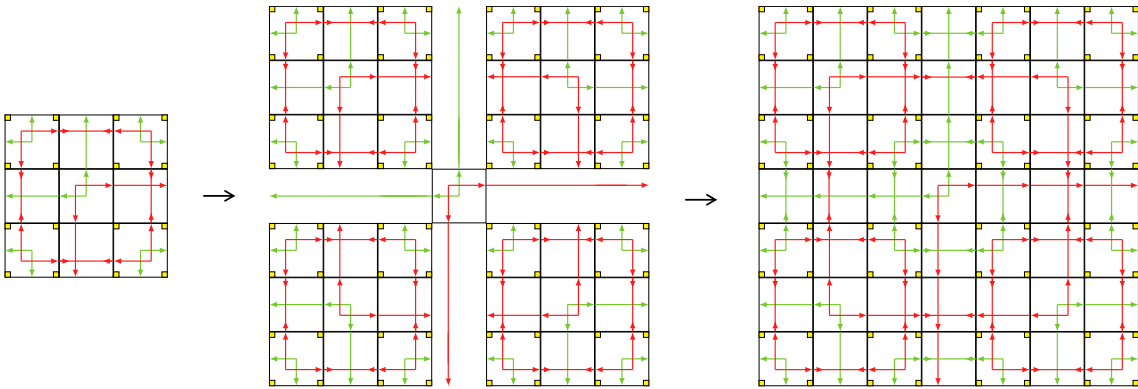


Figure 9: Transformation of  $a_1$  in  $a_2$ .

Observe that for each  $n \in \mathbb{N}$ , macrotiles  $b_n, d_n$  and  $c_n$  can be obtained by rotating  $a_n$  clockwise by  $\frac{\pi}{2}, \pi$  and  $\frac{3\pi}{2}$  radians respectively. Besides that, for each macrotile of rank  $n$ , for any  $m < n$ , macrotiles of rank  $m$  appear periodically in the macrotile of rank  $n$  with vertical and horizontal periods equal to  $2^{m+2}$ . For instance, 0-macrotiles appear in a 2-macrotile with period  $(4, 4)$  (see Figure 9).

Theorem 1 describes all possible Robinson tilings. You can find the proof in [5, 9].

**Theorem 1.** In a valid Robinson tiling of the plane, for each  $n \in \mathbb{N}$ , any occurrence of a  $n$ -macrotile belongs to an occurrence of some  $(n + 1)$ -macrotile.

It turns out that Theorem 1 is still valid in quadrants, instead of full tilings.

**Lemma 1.** Given a valid tiling of a quadrant  $Q$  for any  $n \in \mathbb{N}$  there exists a subquadrant  $Q_n$  of  $Q$  where, for any  $k < n$ , each occurrence of a  $k$ -macrotile is contained in an occurrence of a  $(k + 1)$ -macrotile.

*Proof.* As in Theorem 1. □

A **macrotile grid** of rank  $n$  is a periodic set of  $n$ -macrotiles separated by empty rows of width 1 which can be completed to get a valid tiling of the plane. Macrotile grids of ranks 0 and  $n$  are shown in Figures 10 and 11.

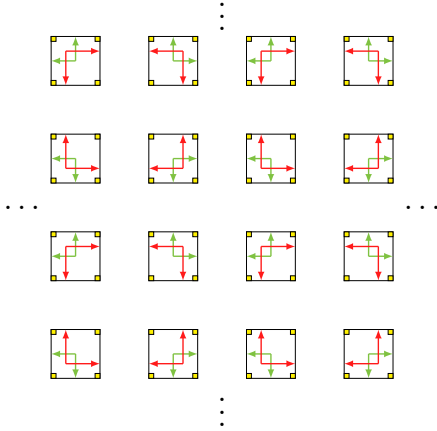


Figure 10: A macrotile grid of rank 0

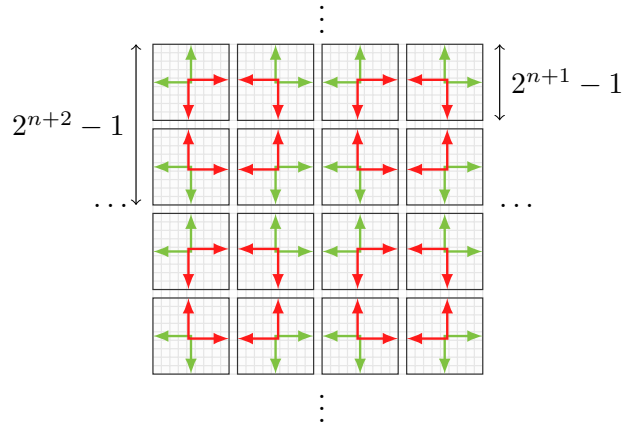


Figure 11: A macrotile grid of rank  $n$

An **infinite vertical (respectively, horizontal) line** for a tiling  $\tau$  of a quadrant  $Q$  is a column (respectively, line) of cells, separating the quadrant in two nonconnected components, all cells of which contain vertical (respectively, horizontal) arrows of the same color and position on the side, while the direction can change. Here is an example of an infinite horizontal line:



**Lemma 2.** For a valid Robinson tiling  $\tau$  of a quadrant  $Q' \subset Q_1$ , if there are no infinite lines in  $Q'$  then there exists a macrotile grid of rank 0 which agrees with the restriction of  $\tau$  to  $Q'$ .

*Proof.* Assume towards a contradiction that there is no 0-macrotile grid agreeing with  $\tau|_{Q'}$ . Since  $\tau$  is valid, for any 4 tiles sharing a corner, one of them is a 0-macrotile. Moreover, since  $Q' \subset Q_1$ , any 0-macrotile is a part of some 1-macrotile.

By our assumption, there is no macrotile grid of rank 0, thus there exists a cell  $(s, t) \in Q'$  containing a 0-macrotile such that one of the following cells:  $(s + 2, t + 1)$ ,  $(s + 1, t + 2)$  contains a 0-macrotile. Indeed, if there is no such cell then for any  $(s, t) \in Q'$  covered with a 0-macrotile, in cells  $(s, t + 1)$ ,  $(s + 1, t + 1)$ ,  $(s + 1, t)$  there are no 0-macrotile because  $\tau$  is valid (by rule  $(::)$ ) and in  $(s + 2, t + 1)$ ,  $(s + 1, t + 2)$  there are no 0-macrotile because of the last assumption. Thus, by local rules, there are 0-macrotilers in cells  $(s + 2, t)$  and  $(s, t + 2)$ . Applying this argument for all cells with 0-macrotilers in  $Q'$ , we get a 0-macrotile grid which yields a contradiction.

Without loss of generality suppose cells  $z_1 = (s, t)$  and  $z_2 = (s + 2, t + 1)$  contain 0-macrotilers (the symmetric case works the same). Both of these tiles are contained in different nonintersecting 1-macrotilers, shifted by 1 vertically. This implies the occurrence of 0-macrotilers in cells  $(s, t + 2)$ ,  $(s, t - 2)$ ,  $(s + 2, t + 3)$ ,  $(s + 2, t - 1)$ , two of which are contained in the same 1-macrotile as the ones from cells  $z_1, z_2$ . Two remaining tiles are contained in two other 1-macrotilers. Going on with these arguments, we get two vertical rows of 1-macrotilers separated by a column of width 1, all tiles of which contain horizontal green arrows. That means all tiles of this column contain vertical arrows of the same color and position on the side which forms a vertical infinite line. Figure 12 illustrates this reasoning. □

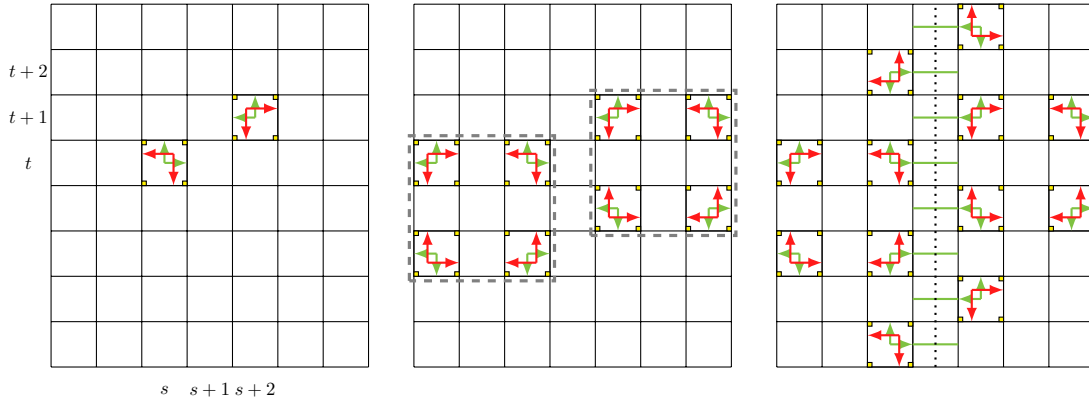


Figure 12: The sketch for the proof of Lemma 2: vertical arrows of the infinite line are denoted by dotted black lines.

**Lemma 3.** Given a valid Robinson tiling  $\tau$  of a quadrant  $Q$ , for any  $n \in \mathbb{N}$  there exists a quadrant  $Q'_n \subseteq Q$  such that there exists a macrotile grid of rank  $n$  which agrees with the restriction of  $\tau$  to  $Q'_n$ .

*Proof.* Let us prove this lemma for  $n = 0$ . Consider  $Q_1$  from Lemma 1, any 0-macrotilde is contained in some 1-macrotilde in  $Q_1$ .

By Lemma 2, it is enough to show that there is a subquadrant of  $Q_1$  that contains no infinite lines. We will prove that there is no more than one infinite line in each direction in  $Q_1$ . It is enough to prove it for vertical lines since the horizontal case is symmetric. Suppose there exist two vertical infinite lines in  $Q_1$  at distance  $h$  from one another. Let  $n = \lceil \log(h + 1) \rceil$ , so that the sides of any  $n$ -macrotilde is longer than  $h$ . Notice that between these infinite lines,  $\tau$  is valid and infinite lines can not intersect macrotildes of finite rank (by construction of the macrotildes). Since the tiling is valid between the lines, for any  $k \in \mathbb{N}$ , each macrotilde of rank  $k$  is a part of some macrotilde of rank  $k + 1$  which is not possible since there are no macrotildes of rank  $n$  between the lines. Thus, there are no more than 2 infinite lines in  $Q_1$  (one vertical and one horizontal). All that remains is to consider a quadrant  $Q' \subset Q_1$  which doesn't contain those lines.

We proved Lemma 3 for the case  $n = 0$ . Since macrotildes of all ranks have the same properties as macrotildes of rank 0, the proof for the general case is the same.  $\square$

Notice that for any  $n$  in  $\mathbb{N}$ , a macrotilde grid of rank  $n$  can be completed to form a macrotilde grid of rank  $n + 1$  in four different ways. Thus for  $m > n$ , a grid of  $n$ -macrotildes is a part of  $4^{m-n}$  different grids of  $m$ -macrotildes.

### 3 Formalizing the growth of Robinson tilings

In this section, we will give a formal definition of growth for Robinson tilings.

Let  $A$  denote the Robinson tileset. From now on we will consider partial tilings, where some cells of the plane are empty. We introduce an additional tile  $\perp$  denoting an absence of tile (an empty cell). Thus, we can define a **partial tiling** of a set  $X \subseteq \mathbb{Z}^2$  as a tiling of  $X$  by tiles from  $A_\perp = A \cup \{\perp\}$ . The set of nonempty cells is called the **domain** of the tiling.

For biological and physical systems, we consider the process of growth as follows: initially, we are given a seed; then as time passes, in the neighborhood of the already grown structure, new particles may be added depending on local circumstances.

We will use the following model: initially we are given a **seed** — a partial tiling with finite domain (there are no restrictions: it can possibly contain tiles violating the Robinson local rules). Then at each step we apply a growth rule for each empty cell; the growth rule can dictate that the cell should remain

empty, that a given tile should be placed, or that an error occurred. The size of the neighborhood and the growth rule are fixed. We will formalize this model with cellular automata.

Recall that a **cellular automaton** on  $\mathbb{Z}^2$  with an alphabet  $A_\perp$  is a function  $A_\perp^{\mathbb{Z}^2} \rightarrow A_\perp^{\mathbb{Z}^2}$ ; it is determined by a neighborhood type and a transition function. A transition function of a cellular automaton working with Moore neighborhoods of radius  $t$  is given by  $f : A_\perp^{(2t+1)^2} \rightarrow A_\perp$ . At each step of the automaton, this function is applied to a neighborhood of each cell of  $\mathbb{Z}^2$  and put the result in this cell. Remark that in each fixed moment of time, a state of such automaton is a partial tiling of the plane and all changes occur depending on a local configuration. That is why we use cellular automata to formalize the growth of tilings.

We will consider automata with an additional symbol  $\top$  denoting an error. If there exists at least one cell in this state, the automaton halts: this allows to report an error in computation immediately. From now on we consider automata whose transition functions look like  $f : A_\perp^{(2t+1)^2} \rightarrow A_{\perp\top}$  where  $A_{\perp\top} = A_\perp \cup \{\top\}$ . If there is the symbol  $\top$  in some cell, then the automaton halts.

Let us define a cellular automaton simulating growth. A transition function  $f : A_\perp^{(2t+1)^2} \rightarrow A_{\perp\top}$  of an automaton working on  $\mathbb{Z}^2$  is called a **growth rule** if for any configuration  $S \in A_\perp^{(2t+1)^2}$ , the following conditions hold:

(\*) A new added cell matches the Robinson local rules with its 8 neighbors:  $f(S)$  is valid in  $S$ 

$(-1,1)$	$(0,1)$	$(1,1)$
$(-1,0)$		$(1,0)$
$(-1,-1)$	$(0,-1)$	$(1,-1)$

.

(\*) The transition function returns an error ( $\top$ ) if and only if  $S$  does not occur in some Robinson tiling of the plane. This means that  $S$  appears in some valid Robinson tiling if and only if  $f(S) \neq \top$ .

A **growth cellular automaton** is a cellular automaton whose transition function is a growth rule. Let us define a partial order on  $A_{\perp\top}$ : for any  $a \in A_\perp$ , we have  $\perp \leq a$  and  $a \leq \top$ . If  $a, b \in A$ , then  $a$  and  $b$  are incomparable.

Let us now consider a partial order on partial tilings of  $t$ -neighborhoods. Given  $S, S' \in A_\perp^{(2t+1)^2}$ , we say that  $S \leq S'$  if and only if

$$\forall z \in (2t+1)^2, S(z) \leq S'(z)$$

In other words,  $S \leq S'$ , when the domain of  $S$  is a subset of the domain of  $S'$  and they agree on the domain of  $S$ .

A function  $f : A_\perp^{(2t+1)^2} \rightarrow A_{\perp\top}$  is a **nondecreasing growth rule** if for any  $S, S' \in A_\perp^{(2t+1)^2}$  such that  $S \leq S'$ , we have  $f(S) \leq f(S')$ .

Intuitively, we can consider the information contained in each configuration: if we fill some empty cell in a configuration, the amount of information in this configuration increases. Thus, having a nondecreasing growth means that if with a given amount of information, we decide to add a particular tile, then having strictly more information we should keep our decision (or return an error).

Suppose we are given two configurations  $S_1$  and  $S_2$  of a  $t$ -neighborhood with domains  $D_1$  and  $D_2$  respectively.  $S_1$  and  $S_2$  are **compatible** if they agree on the intersection of their domains:  $S_1|_{D_1 \cap D_2} = S_2|_{D_1 \cap D_2}$ . Let us define the union operation for two compatible configurations  $S_1, S_2$ :

$$(S_1 \cup S_2)(z) := \begin{cases} S_1(z) & z \in D_1 \\ S_2(z) & z \in D_2 \setminus D_1 \end{cases}$$

**Lemma 4.** Let  $S_1, S_2$  be a pair of compatible configurations of  $t$ -neighborhood and a nondecreasing growth function  $f$ . If  $f(S_1), f(S_2) \in A$  and  $f(S_1) \neq f(S_2)$  then  $f(S_1 \cup S_2) = \top$ . That means, if a growth rule returns two different tiles from  $A$  on two compatible configurations then the union of these configurations never occurs in a valid Robinson tiling of the plane.

Suppose  $f(S_1), f(S_2) \in A$  and  $f(S_1) \neq f(S_2)$ . In this case, since  $f$  do not decrease:  $f(S_1 \cup S_2) \geq f(S_1)$ . Thus,  $f(S_1 \cup S_2) \in \{f(S_1), \top\}$ . The same holds for the second configuration:  $f(S_1 \cup S_2) \in \{f(S_2), \top\}$ . And since  $f(S_1) \neq f(S_2)$ , we get that  $f(S_1 \cup S_2) = \top$ .  $\square$

## 4 Robinson tilings do not grow

We are interested in whether a tiling can grow to cover the whole plane. Given an initial configuration, a growth cellular automaton **eventually covers the plane** if for any cell  $x \in \mathbb{Z}^2$ , there exists a moment of time when the automaton put a tile in this cell. Notice that, if during the execution of an automaton an error occurs, then it doesn't cover the plane.

**Theorem 2.** There is no cellular automaton with nondecreasing growth rule which, working on some initial configuration, eventually covers the plane.

To prove this theorem, we will reason by contradiction: suppose there exists an automaton with  $t$ -neighborhood ( $t > 0$ ) and a seed such that it eventually covers the whole plane. We will show that in this case, there exist two compatible configurations of  $t$ -neighborhoods on which the growth rule returns two different tiles and the union of which occurs in some valid Robinson tiling. This will contradict Lemma 4.

### 4.1 The base of the proof

Let  $\tau$  denote the tiling of the plane eventually generated by the growth automaton. Consider a quadrant  $Q$  not containing the seed. Notice that the tiling is valid on  $Q$ : indeed, assume towards a contradiction that there is a tile which is not legal in respect to the configuration of its 1-neighborhood  $S$ . In this case, the last added tile among tiles in  $S$  was not valid in its 1-neighborhood which contradicts point (\*) from the definition of the growth rule.

Let  $n = \lceil \log t \rceil + 2$ . A  $t$ -neighborhood is not bigger than an  $(n-1)$ -macrotile:  $2^n - 1 = 2^{\lceil \log t \rceil + 2} - 1 \geq 4t - 1 \geq 2t + 1$ , because  $t \geq 1$ . Thus a  $t$ -neighborhood can not intersect more than 4 different  $(n-1)$ -macrotiles from a macrotile grid. Since  $\tau$  is valid on  $Q$ , there exists a quadrant  $Q_{n+3}$  so that  $\tau|_{Q_{n+3}}$  agrees with some  $(n+3)$ -macrotile grid. We call  $G_n$  the subset of  $\mathbb{Z}^2$ , where a grid of  $n$ -macrotiles compatible with  $\tau|_{Q_{n+3}}$  is defined (such a grid exists since it is a subset of the  $(n+3)$ -grid defined above).

Let  $A_{n+3}$  denote an occurrence of a macrotile  $a_{n+3}$  in  $Q_{n+3}$ . Denote by  $Y$  the vertical coordinate of its central cell; denote by  $X$  the horizontal coordinate of the central cell of an occurrence of  $b_{n+2}$  in  $A_{n+3}$ . From now on we will work with cells of the quadrant  $Q_{XY}$ . This construction is shown in Figure 13. Here and later in figures we denote types of macrotiles as follows: the size of font is proportional to the rank of a macrotile. In Figure 13, the  $n$ -macrotiles from the grid on  $G_n$  are denoted by gray font, the  $(n+2)$ -macrotiles  $a_{n+2}, b_{n+2}, c_{n+2}, d_{n+2}$  are marked by orange and denoted by black larger font, the  $A_{n+3}$  macrotile is filled with yellow and is denoted by the largest font.

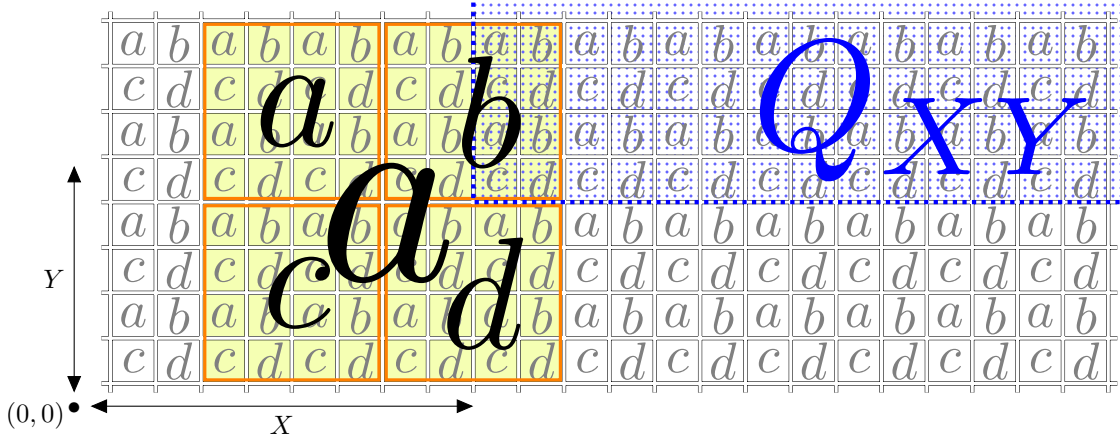


Figure 13: The grid of  $n$ -macrotiles,  $A_{n+3}$  (filled with yellow), and the quarter  $Q_{XY}$  (filled with blue dots).

Recall that  $B_t(z)$  denotes a  $t$ -neighborhood of a cell  $z \in \mathbb{Z}$ . For any set  $X \subseteq \mathbb{Z}^2$ , we write  $\overline{X}$  for  $\mathbb{Z}^2 \setminus X$ . Let  $E$  denote the set of all cells from  $Q_{XY}$  not contained in  $G_n$ :  $E := Q_{XY} \cap \overline{G_n}$ . For any cell



$z$ , let  $B_t^{\overline{E}}(z) := B_t(z) \cap \overline{E}$ , we will call this set a  **$\overline{E}$ -neighborhood** of  $z$ . Sets  $E$  and  $B_t^{\overline{E}}(z)$  are shown in Figure 14.

In Section 4.2, we will prove the following statement:

**Lemma 5.** For any cell  $z$  in  $E$ , for a configuration  $S = \tau|_{B_t^{\overline{E}}(z)}$ , there exist two cells in  $Q_{XY}$  containing different tiles in  $\tau$  whose  $\overline{E}$ -neighborhoods are compatible with  $S$ . We will call these cells **twins** of  $z$ .

Figure 14 illustrates Lemma 5.

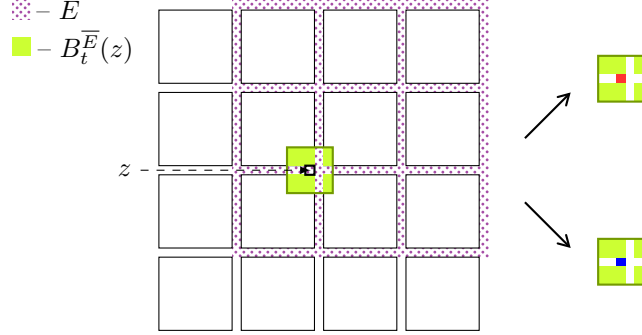


Figure 14: Twins for a cell  $z$ .

Now we show that this fact implies Theorem 2. Let  $u$  denote the cell which was added the first among cells from  $E$  during the growth process. Let  $U$  denote the configuration of  $B_t(u)$  at the moment just before the tile was added. All cells in  $E$  are empty in  $U$  since  $u$  is the first added tile in  $E$ . Let  $U' := \tau|_{B_t^{\overline{E}}(u)}$ . Let  $v$  denote a twin of  $u$  such that  $\tau(u) \neq \tau(v)$ . Let  $V$  denote the configuration of  $B_t(v)$  at the moment just before  $v$  was filled with a tile. We get the following:

$$f(U) = \tau(u) \neq \tau(v) = f(V)$$

At the same time,  $V$  is compatible with  $U'$  which is compatible with  $U$  since  $U = U \cap U'$ ; then  $V$  is compatible with  $U$ . Moreover,  $V \cup U$  is a subconfiguration of  $\tau|_{B_t(v)}$  and  $B_t(v) \subset Q$ , thus  $V \cup U$  occurs in a valid Robinson tiling which contradicts Lemma 4.

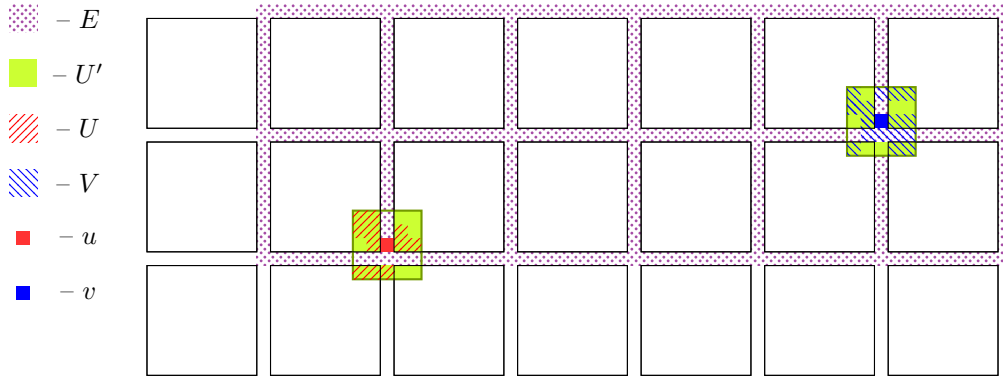


Figure 15: The first filled cell in  $E$  and its twin.

Thus, proving Lemma 5 is all that rests to prove Theorem 2.

## 4.2 Looking for twins: proof of Lemma 5

Our aim is to find twins in  $Q_{XY}$  for each cell of  $E$ . We will consider cells separately depending on their  $\overline{E}$ -neighborhoods. We distinguish cells  $z$  for which  $B_t^{\overline{E}}(z) \subset G_n$  (for instance, two right-hand cells

in Figure 16) and cells for which this doesn't hold (two left-hand cells in Figure 16). The cells of the first type form a set  $E_{G_n} := \{z \mid B_t^{\bar{E}}(z) \subset G_n\}$ ; the remaining cells form  $E \setminus E_{G_n}$ . These two sets are illustrated by Figure 17.

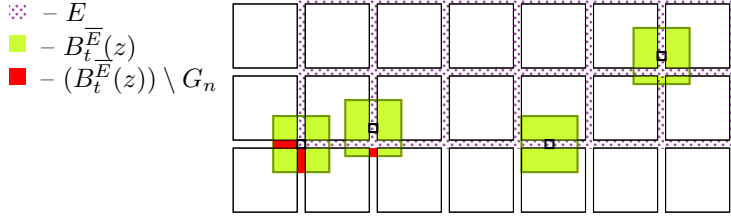


Figure 16: The  $\bar{E}$ -neighborhoods of two right-hand cells are in  $G_n$ , while for two left-hand cells it doesn't hold.

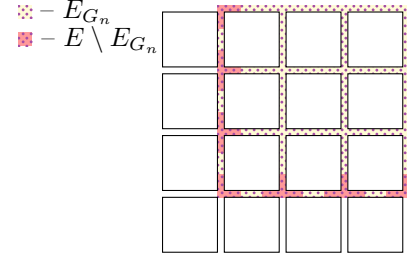


Figure 17: Sets  $E \setminus E_{G_n}$ ,  $E_{G_n}$  and the grid of  $n$ -macrotiles.

We will first show that Lemma 5 holds for cells in  $E_{G_n}$ .

#### 4.2.1 When the cell $z$ is in $E_{G_n}$

The partial tiling  $\tau|_{G_n}$  has vertical and horizontal periods equal to  $2^{n+2}$  (See Figure 11). Thus, to prove Lemma 5 for all cells in  $E_{G_n}$ , it is enough to prove it for all cells of any  $(2^{n+2} \times 2^{n+2})$ -square from  $\{(x, y) \mid (x - t, y - t) \in Q_{XY}\}$ .

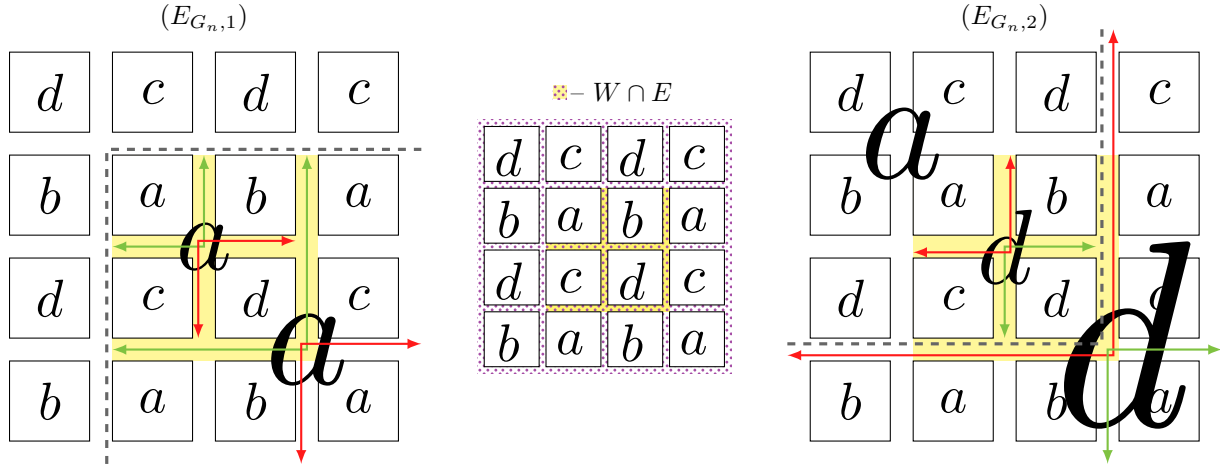


Figure 18: Twins for cells in  $W \cap E$  in the case  $E_{G_n}$ .  $W \cap E$  is filled with yellow; the gray dashed line is a border of a  $(n + 2)$ -macrotile.

Consider a  $2^{n+2} \times 2^{n+2}$ -square  $W$ , containing four  $n$ -macrotiles, so that they can be completed to form a  $(n + 1)$ -macrotile, one row on the bottom of them and one column to the right of them, as it's shown in Figure 18: cells in  $E \cap W$  are filled with yellow.

Consider two variants to complete the  $n$ -macrotile grid to  $(n + 3)$ -macrotile grid. In the first case denoted by  $(E_{G_n,1})$ , four  $n$ -macrotiles from  $W$  are contained in  $a_{n+1}$  which is contained in  $a_{n+2}$  (Figure 18, the left part). In the second case  $((E_{G_n,2})$  in Figure 18),  $n$ -macrotiles from  $W$  are contained in  $d_{n+1}$  which is contained in  $a_{n+2}$  which is contained in  $d_{n+3}$ .

Each cell in  $W \cap E$  contains different tiles in cases  $(E_{G_n,1})$  and  $(E_{G_n,2})$ . Each of these cases is a part of some  $(n + 3)$ -macrotile, thus, they both occur in  $Q_{XY}$  infinitely many times. Thence, any cell in  $W \cap E$  has twins in  $Q_{XY}$ , which concludes the proof for the cells in  $E_{G_n}$ .

### 4.2.2 When the cell $z$ is in $E \setminus E_{G_n}$

By definitions of  $n$  and  $E_{G_n}$ , a  $t$ -neighborhood of a cell in  $E \setminus E_{G_n}$  intersects either two or three  $(n-1)$ -macrotils from  $\overline{Q_{XY}}$ . We will classify cells in  $E \setminus E_{G_n}$  depending on which  $(n-1)$ -macrotils from  $\overline{Q_{XY}}$  are intersected by their neighborhoods. We get three classes which are shown in Figure 19:  $(^db)$ ,  $(^dba)$  and  $(ba)$ .

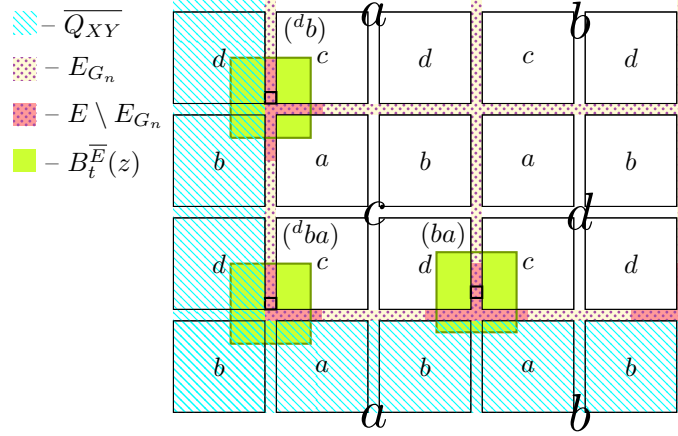


Figure 19: The grid of  $(n-1)$ -macrotils (the smallest font) and three classes of  $E_{G_n}$  cells.

### 4.2.3 Case $(ba)$

Suppose the  $\overline{E}$ -neighborhood of a cell in  $E \setminus E_{G_n}$  intersects two  $(n-1)$ -macrotils from  $\overline{Q_{XY}}$ :  $b_{n-1}$  on the left and  $a_{n-1}$  on the right. Then the column between these macrotils could be filled differently, it depends on the macrotils of higher ranks. All possible fillings of the column are displayed in Figure 20. We denote each case by an arrow and one or two letters: the arrow shows the direction of the arrow in the column and the letters are types of macrotils in centers of which this arrow could begin. For example,  $(\downarrow^b)$  denotes the case where the arrow is directed downwards and could come from the center of a  $b$ -macrotile (note that between  $(\downarrow^a)$  and  $(\downarrow^b)$ , the horizontal positions of the red arrows are different);  $(\uparrow_{a,b})$  denotes the upwards arrow coming from a macrotile of type  $a$  or  $b$  (their upwards arrows are the same).

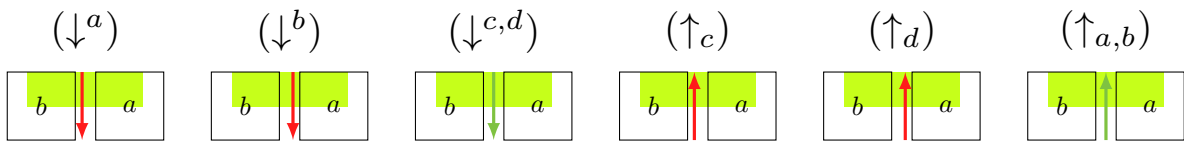


Figure 20: Variants of columns between  $b_{n-1}$  and  $a_{n-1}$ , intersected by  $B_t^{\overline{E}}(z)$  in case  $(ba)$ .

First we consider the case where the arrow in the column is directed downwards. Figure 21 shows two twins in case  $(\downarrow^a)$ . On the left,  $b_{n-1}$  and  $a_{n-1}$  are contained in  $a_{n+1}$ ; on the right, they are contained in two different  $(n+1)$ -macrotils  $c_{n+1}$  and  $d_{n+1}$  which are both contained in  $a_{n+2}$ . For two these configurations, the arrow is the same in the column between  $b_{n-1}$  and  $a_{n-1}$ , while all possible central cells of neighborhoods contain different tiles in different configurations. The same reasoning applies for cases  $(\downarrow^b)$  and  $(\downarrow^{c,d})$ : they are shown in Figures 25 and 26 in the Appendix.

In Figure 21 and later the considered cells  $z$  are filled with yellow: ; the union of sets  $B_t^{\overline{E}}(z) \cap \overline{Q_{XY}}$  for those  $z$  is marked with light green: .

The only cases left are those where the arrow in the column is directed upwards. Figure 22 displays twins for cases  $(\uparrow^c)$  (on the left) and  $(\uparrow^d)$  (on the right). In the configuration  $(\uparrow_{c1})$ ,  $b_{n-1}$  intersected

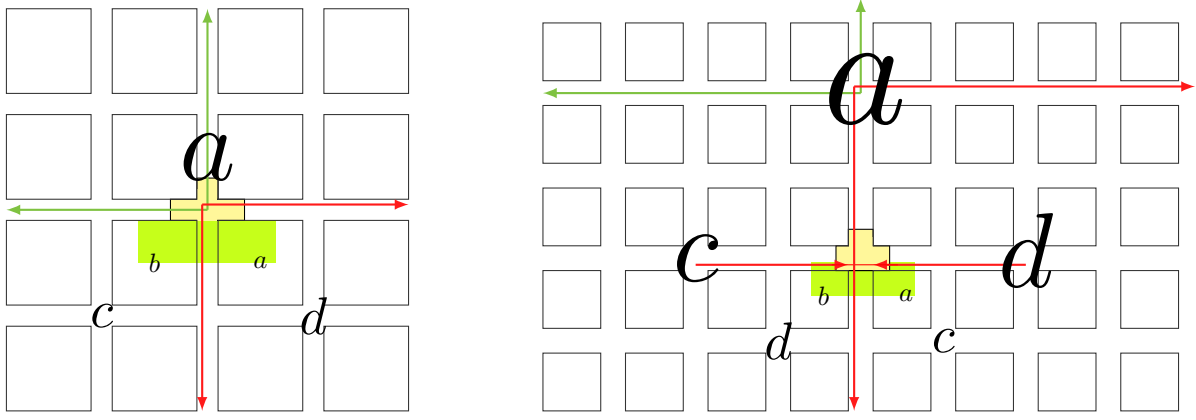


Figure 21: Twins for the case where the arrow between  $b_{n-1}$  and  $a_{n-1}$  is  $(\downarrow^a)$ .

by  $B_t^{\overline{E}}(z)$  is a part of an occurrence of  $b_n$  which is contained in  $a_{n+1}$  which is located in  $c_{n+2}$  which is eventually a part of  $d_{n+3}$ , while  $a_{n-1}$  is a part of an occurrence of  $a_n$  which is in  $b_{n+1}$  which is located in the considered above occurrence of  $c_{n+2}$ . In the configuration  $(\uparrow_{c2})$ ,  $b_{n-1}$  intersected by  $B_t^{\overline{E}}(z)$  is a part of an occurrence of  $d_n$  which is contained in  $a_{n+1}$  from  $(\uparrow_{c1})$ , while  $a_{n-1}$  is a part of an occurrence of  $c_n$  which is contained in the occurrence of  $b_{n+1}$  considered in  $(\uparrow_{c1})$ .

The arrow in the vertical column in both cases is the middle arrow of  $c_{n+2}$ . For each cell  $z$  in the considered area, the tiles contained in this cell are different in two configurations. Configurations  $(\uparrow_{d1})$  and  $(\uparrow_{d2})$  work the same.

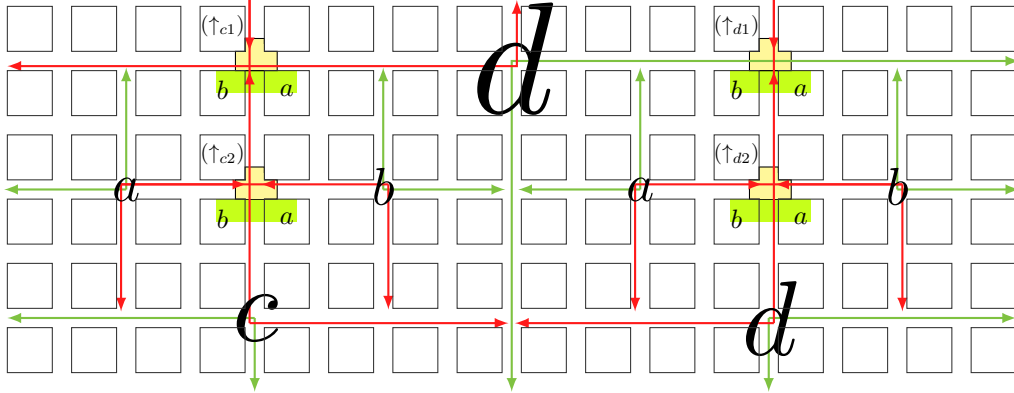


Figure 22: Twins for cases  $(\uparrow_c)$  and  $(\uparrow_d)$ .

For the last case,  $(\uparrow_{a,b})$ , the twins are shown in Figure 23.

#### 4.2.4 Case $(^db)$

As we already mentioned, for all  $N$ , all  $N$ -macrotiles are rotations of  $a_N$ . Thus, configurations with twins for the case  $(^db)$  can be obtained by rotating the configurations from the case  $(ba)$  by  $90^\circ$ .

#### 4.2.5 Case $(^dba)$

There is the only case where  $B_t^{\overline{E}}(z)$  intersects three  $(n-1)$ -macrotiles from  $\overline{Q_{XY}}$ : these macrotiles are located around the origin of  $Q_{XY}$  and the arrows in a line and a column between  $d_{n-1}$ ,  $b_{n-1}$  and  $a_{n-1}$  are as it's shown in Figure 24. The twins for this case are displayed in the same figure: for any  $z$

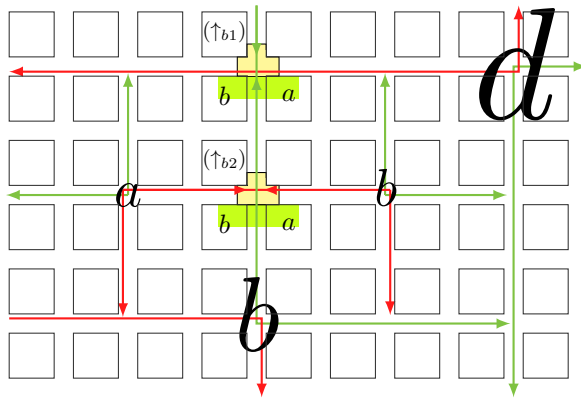




Figure 23: Twins for the case  $(\uparrow_{a,b})$ .

from the considered area, it contains two different tiles for configurations  $({}^d b a_1)$  and  $({}^d b a_2)$ . Indeed, each cell touching the top side of  $a_{n-1}$ , except the one in the corner, contains tiles with arrows of opposite directions in these two configurations; the same is true for the cells touching the right side of  $d_{n-1}$ . The remaining cell is the one in the corner; in the configuration  $({}^d b a_1)$  it contains , while in  $({}^d b a_2)$  it contains .

Thence, we covered all the cases which means that twins exist for each cell  $z$  in  $E$ : Lemma 5 is true. □

This proves Theorem 2. □

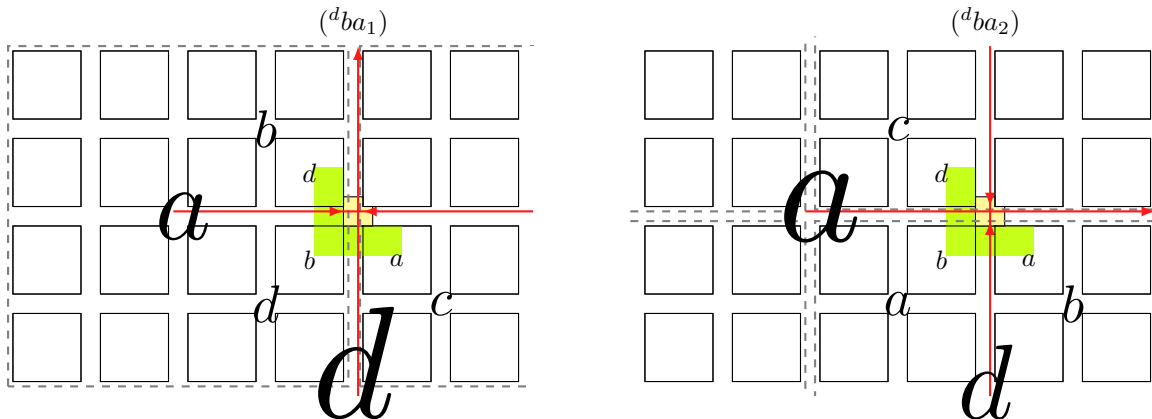


Figure 24: Twins in the case  $({}^d b a)$ . Borders of  $(n+2)$ -macrotiles are marked by the gray dashed line.

## 5 Conclusion

### 5.1 Future work

We modeled the growth of Robinson tilings with cellular automata satisfying conditions  $(*)$  and  $(\odot)$  with a nondecreasing growth rule. However, we conjecture that all restrictions except  $(*)$  are unnecessary for this result. Thus, obtaining the same result with weaker conditions (or showing a counterexample) would be a good continuation of this work.

Besides that, the growth model could be generalized, for instance, in a probabilistic way. For this, it is enough to consider probabilistic cellular automata; this approach is more realistic for modeling physical and chemical processes.

Our result shows that there exists a hierarchical tiling of the plane that can not be grown. The question is still open for many other tilings and should be investigated in order to find connections between growing and other properties of a tileset (for instance, entropy of the dynamical system).

## 5.2 Other activities

During my internship, besides the research described in this report, I participated in the local scientific life. In June, I took part in the on-place organization of the CSR conference (<https://logic.pdmi.ras.ru/csr2018/welcome>). Besides that, I was a coauthor of a course on Tilings and Computations in the summer school “Contemporary Mathematics” (<https://www.mccme.ru/dubna/eng/>). I gave two lectures out of four, made exercise sheets, and took part in writing lecture notes (all these materials can be found here: <https://www.mccme.ru/dubna/2018/courses/gamard-pchelina.html>).

## References

- [1] Robert Berger. The undecidability of the domino problem. *Memoirs of the American Mathematical Society*, 66, 1966.
- [2] Karel Culik. An aperiodic set of 13 Wang tiles. *Discrete Mathematics*, 160(1):245–251, 1996.
- [3] David Doty. Theory of Algorithmic Self-assembly. *Communications of the ACM*, 55(12):78–88, 2012.
- [4] Bruno Durand, Leonid A. Levin, and Alexander Shen. Complex tilings. *J. Symbolic Logic*, 73(2):593–613, 2008.
- [5] Thomas Fernique. Yet Another Proof of the Aperiodicity of Robinson Tiles. <http://arxiv.org/abs/1506.06492>.
- [6] U. Grimm and D. Joseph. Modeling Quasicrystal Growth. *Quasicrystals: An Introduction to Structure, Physical Properties and Application*, page 199, 2002.
- [7] Emmanuel Jeandel and Michaël Rao. An aperiodic tileset of 11 Wang tiles. <https://arxiv.org/abs/1506.06492>, 2015.
- [8] Jarkko Kari. A small aperiodic set of Wang tiles. *Discrete Mathematics*, 160(1-3):259–264, 1996.
- [9] Daria Pchelina and Guilhem Gamard. Computations: from Turing Machines to Tiling. <https://www.mccme.ru/dubna/2018/notes/gamard-pchelina-notes.pdf>, 2018.
- [10] Roger Penrose. The role of aesthetics in pure and applied mathematical research. *Bulletin of the Institute of Mathematics and its Applications*, 10:266, 1974.
- [11] Raphael M. Robinson. Undecidability and nonperiodicity for tilings of the plane. *Inventiones Mathematicae*, 12(3):177–209, 1971.
- [12] Joshua E.S. Socolar. Growth Rules For Quasicrystals. *Quasicrystals: The State of the Art*, pages 325–359, 1999.
- [13] Hao Wang. Proving theorems by pattern recognition—II. *Bell System Technical Journal*, 40:1–41, 1961.

## Appendix: additional figures

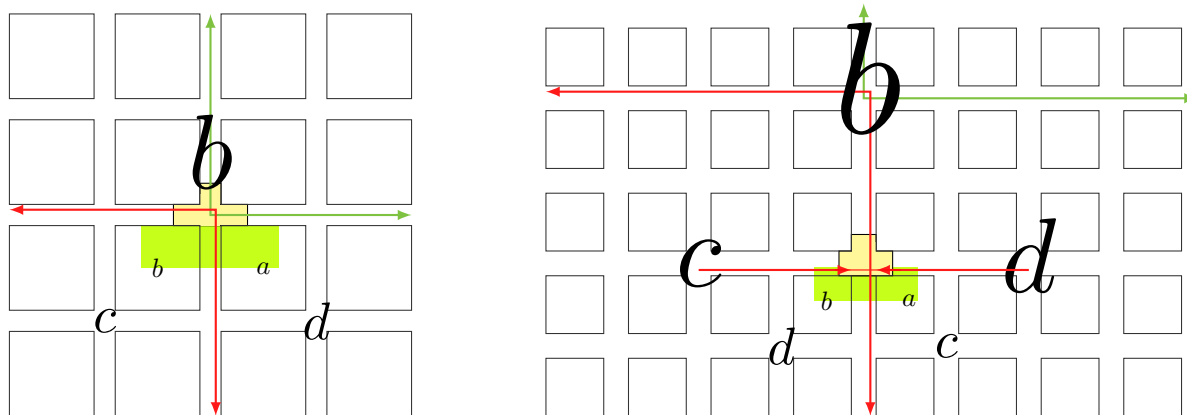


Figure 25: Twins for cells  $z$  is in  $E \setminus E_{G_n}$ , case  $(ba)$ , where the arrow between  $b_{n-1}$  and  $a_{n-1}$  is  $(\downarrow^b)$ .

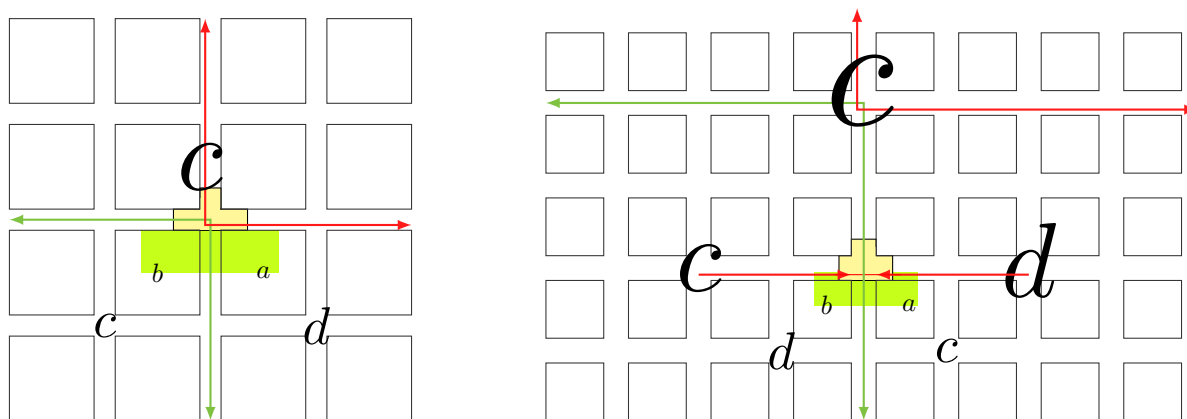


Figure 26: Twins for cells  $z$  is in  $E \setminus E_{G_n}$ , case  $(ba)$ , where the arrow between  $b_{n-1}$  and  $a_{n-1}$  is  $(\downarrow^{c,d})$ .